**Atmospheric
Chemistry
and Physics**

European summer surface ozone 1990–2100

J. Langner, M. Engardt, and C. Andersson

Swedish Meteorological and Hydrological Institute, 601 76, Norrköping, Sweden

Correspondence to: J. Langner (joakim.langner@smhi.se)

Abstract. The impact of climate change and changes in ozone precursor emission on summer surface ozone in Europe was studied using a regional CTM over the period 1990 to 2100. Two different climate simulations under the SRES A1B scenario together with ozone precursor emission changes from the RCP4.5 scenario were used as model input. In southern Europe regional climate change leads to increasing surface ozone concentrations during April–September, but projected emission reductions in Europe have a stronger effect, resulting in net reductions of surface ozone concentrations. In northern Europe regional climate change decreases surface O_3 and reduced European emissions acts to further strengthen this trend also when including increasing hemispheric background concentrations. The European O_3 precursor emission reductions in RCP4.5 are substantial and it remains to be seen if these reductions can be achieved. There is substantial decadal variability in the simulations forced by climate variability which is important to consider when looking at changes in surface O_3 concentrations, especially until the first half of the 21st century. In order to account for changes in background O_3 future regional model studies should couple global (hemispheric) and regional CTMs forced by a consistent set of meteorological and precursor emission data.

1 Introduction

Surface ozone (O_3) has negative effects on human health and vegetation. Background levels of O_3 in the troposphere over the northern mid-latitudes have increased by a factor of two to three since the end of the 19th century (Parrish et al., 2009). This is to a large extent related to increasing man made emissions of O_3 precursors such as methane (CH_4), carbon monoxide (CO), nitrogen oxides (NO_x) and

non-methane volatile organic compounds (NMVOC) (Isaksen et al., 2009). O_3 in the lower troposphere is also regulated by climatic factors such as temperature and solar radiation as well as by surface deposition which in the case of vegetated surfaces is again regulated by temperature, solar radiation, humidity and soil water availability (Jacob and Winner, 2009; Andersson and Engardt, 2010). Given that projections of future climate in Europe indicate substantial changes in these variables there is concern about increasing concentrations of O_3 due to climate change (Royal Society, 2008).

Several studies with regional chemistry transport models have pointed out the importance of climate change for future surface O_3 in Europe (e.g. Langner et al., 2005; Meleux et al., 2007; Engardt et al., 2009; Andersson and Engardt, 2010; Katragkou et al., 2011). The previous studies based their analysis on simulations over time slices of 10–30 yr for current and future climate. In most cases climate projections based on one global climate model was used. The purpose of the present study is to extend the analysis of future changes in surface O_3 in Europe to include the combined transient effects of changes in climate, changes in O_3 precursor emissions and changes in background concentrations over the 110-yr period from 1990 to 2100. We use recent compilations of historic and future trends of emissions of air pollutants over Europe and climate projections from two different global climate models downscaled over Europe to show regional detail.

Section 2 provides details on the setup of the current study including general information on the utilized climate and chemistry transport models. Section 2 also contains an evaluation of the modelling systems' ability to reproduce surface O_3 concentrations in Europe. In Sect. 3 we present the results. We focus on summer (April–September) mean and mean of daily maximum (daily max) concentrations of O_3. Summer is the main growing season and also when surface

O_3 is at its maximum in Europe and hence this period is of main interest for impacts on human health and vegetation. Finally we present conclusions in Sect. 4.

2   Methods and data

To simulate the evolution of surface ozone over Europe during the period 1990–2100 we make use of a chain of models starting with global climate models (GCMs) that feeds boundary conditions into a regional climate model (RCM) with higher spatial resolution over Europe. The resulting meteorological output from the RCM is then used to drive the simulation of emissions, transport, atmospheric chemistry and deposition of air pollutants in a chemistry transport model (CTM) over Europe.

2.1   Climate projection

In order to investigate the uncertainty related to the choice of GCM in projecting future climate change we used results downscaled by a RCM from two different GCMs; the ECHAM5 model (Roeckner at al., 2006) and the HadCM3 model (Collins et al., 2010). Both climate projections used in this study were derived using the SRES A1B scenario (Nakićenović et al., 2000). The RCM used was the Rossby Centre Regional Climate model version 3, RCA3. Model description and evaluation of both current and future climate simulated with RCA3 is given by Samuelsson et al. (2011) and Kjellström et al. (2011). They show that the simulation of past climate using ERA40 as forcing on the boundaries show improvements in the climate simulated by RCA3 compared to previous versions of the model. Remaining model biases include underestimate of the diurnal temperature range over northern Europe in summer and overestimates of precipitation and surface evaporation in northern Europe in the summer (Samuelsson et al., 2011). When using GCM input to drive the simulations for the control period (1961–1990) using boundaries from HadCM3 gives lowest bias compared to observations while the simulation using ECHAM5 is generally too cold and too wet in northern Europe in summer (Kjellström et al., 2011). The climate as downscaled by RCA3 carries on broad features of the climate simulated by the parent GCM. The projection downscaled from HadCM3 has an average temperature change of 2.9 °C between the periods 1961–1990 and 2040–2070 for the European domain while the corresponding value for the projection downscaled from ECHAM5 is 2.0 °C. The HadCM3 projection thereby has the second highest temperature change in an ensemble of 16 projections downscaled from different GCM runs by RCA3 over Europe by Kjellström et al. (2011) while the ECHAM5 projection has the fourth lowest. Both climate projections show an increase in summer precipitation in large parts of northern Europe extending also to south-east over Poland and Belarus between the periods 1990–2009 and

2040–2959 while precipitation generally decrease in southern and south-western Europe. Connected to this is also a summer total cloudiness increase in northern Europe and decrease in southern Europe with the same spatial pattern as for precipitation. The reduction of precipitation in summer is larger in south-western Europe in ECHAM5 and consequently also changes in cloud cover and soil moisture. These factors are important for ozone production and dry deposition to vegetation. Six-hourly meteorological output on 21 model levels, as well as a range of output variables at the surface, was stored from the RCA3 simulations to be used in the CTM modelling.

2.2   Regional chemistry transport model

We used the regional, off-line, Eulerian CTM, MATCH, to simulate the evolution of O_3 and a range of other air pollutants over Europe. The model structure, boundary layer parameterization, advection scheme and numerical treatment are given by Robertson et al. (1999). The chemical scheme in MATCH is based on Simpson et al. (1993), with extensions described by Andersson et al. (2007). The dry deposition of gases and aerosols is calculated using a resistance approach depending on land surface type and for gases the deposition to vegetated surfaces is coupled to soil moisture, temperature, vapour pressure deficit and photosynthetically active radiation (PAR) as described in Andersson and Engardt (2010). The wet scavenging is assumed to be proportional to the precipitation intensity for most gaseous and aerosol components. For O_3, hydrogen peroxide and sulfur dioxide in-cloud scavenging is calculated assuming Henry's law equilibrium; sub-cloud scavenging is neglected for these species. Important model parameters, such as dry deposition velocities and scavenging coefficients are tabulated in Andersson et al. (2007). The model domain covers Europe and part of the North Atlantic using a rotated latitude/longitude grid with 85 by 95 cells and a horizontal resolution of 0.44° by 0.44° (ca. 50 by 50 km). In the vertical direction, the CTM domain reaches 5–6 km above the surface using 15 model levels. The lowest model layer is ~ 60 m thick, increasing to ~ 700 m in layer 15. The temporal resolution of the meteorological input data is six hours, interpolated to one hour in MATCH; the overall model time step is ten minutes.

2.3   Emission data

Anthropogenic emissions of NO_x, sulfur dioxide, ammonia, NMVOC and CO used in the MATCH simulations were taken from the RCP4.5 scenario (Thomson et al., 2011; Lamarque et al., 2010). The RCP scenarios have been developed as a replacement of the SRES scenarios and are now the basis for current modelling activities in the climate modelling community. There are four RCP scenarios corresponding to total anthropogenic radiative forcing estimated to 2.6, 4.5, 6 and 8.5 Wm^{-2} respectively in the year 2100. The RCP data

base provides global gridded historic anthropogenic emissions and scenarios for future emissions for different sectors and pollutants geographically resolved on a 0.5° by 0.5° latitude-longitude grid. Emission estimates are available for every ten years and for use in the CTM modelling we linearly interpolated this data to yearly resolution. It should be noted that the RCP scenarios assume more aggressive air pollution abatement measures and correspondingly larger decreases in O_3 precursors both in Europe and globally compared to e.g. the SRES scenarios. The extent to which such decreases could be achieved is debated (Fiore et al., 2012). Aggregated over the European CTM domain NO_x, NMVOC and CO emissions decrease by 53, 22 and 17 % respectively, from year 2000 to 2050. The decrease is however not uniform. Looking specifically at the changes between 2000 and 2020 we find that emissions decrease by 50–60 % for NO_x in e.g. Germany, Italy, France, Spain and UK, while emissions decrease by more than 80 % in Russia and Ukraine. Wild fire emissions were not included in the simulation and the VOC speciation was constant with time.

Global emissions of CO_2 and methane for 2050 are 45 and 37 % larger respectively in SRES A1B, used in the climate projections, than in the RCP4.5 emission scenario used in the CTM modelling. Global emissions of NO_x and NMVOC for 2050 are 65 and 46 % larger respectively in SRES A1B than in RCP4.5. SRES A1B therefore corresponds to a world with substantially larger emissions of both long-lived greenhouse gases and air pollutants. For the climate change projections this is not so important for the first half of the 21st century where already committed emissions of long-lived greenhouse gases dominate the radiative forcing while towards the end of the century the climate change signal under the RCP4.5 scenario would be expected to be smaller than for SRES A1B. For Europe emission reductions of air pollutants in the RCP4.5 until 2020 are comparable to e.g. the PRIMES base line scenario by IIASA (Amann et al., 2010) for NO_x but smaller for VOC.

Emissions of biogenic isoprene are calculated online in MATCH following Simpson et al. (1995). The isoprene source strength is a function of vegetation type (i.e. tree species), local temperature and PAR. The calculated isoprene emissions increase with PAR and temperature, which are from the driving regional climate model. The relative proportion of the different tree species in each grid cell remains the same throughout all model scenarios. There is currently no treatment of natural sources of nitrogen in MATCH.

2.4   Boundary conditions

Boundary conditions of the chemical components simulated by MATCH were held at current levels (ca. year 2000) in the simulations, with a monthly, horizontal and vertical variation as described in Andersson et al. (2007). For O_3, lateral boundary conditions are based on back-trajectory analyzed measurement data from the EMEP network for year
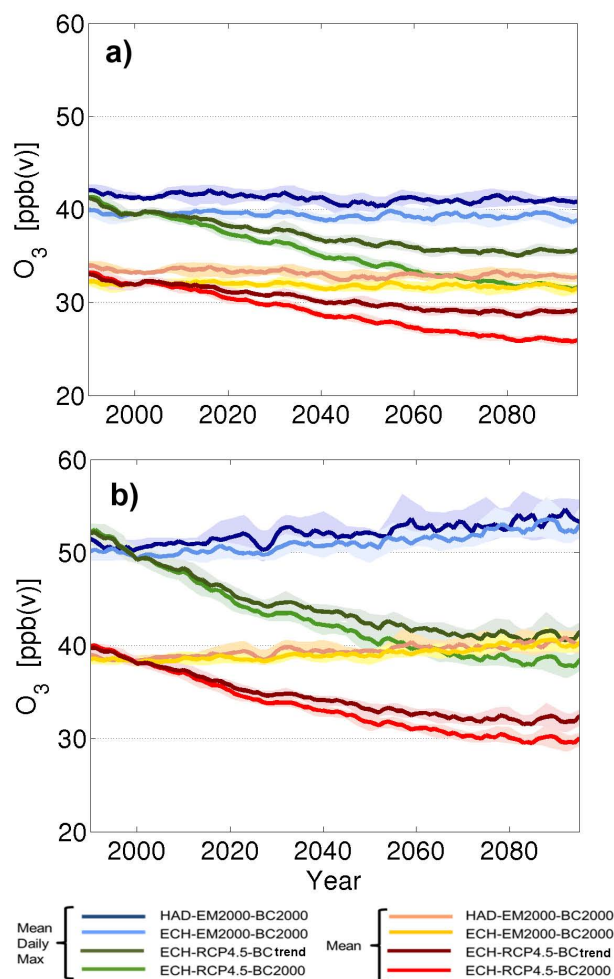
Fig. 1. Simulated geographical-average evolution of summer (April–September) mean surface O_3 concentration and summer mean of daily maximum surface O_3 concentration from 1990 to 2100. Results are **(a)** for the European land area north of 50° N and **(b)** south of 50° N. Thick lines correspond to a 5-yr running mean and the shaded areas correspond to the interval between the 5-yr running mean of the minimum and maximum summer mean values.

1999 and for the top boundary on ozone sonde data from Ireland, UK and Norway for the period 1996–2001 (Andersson et al., 2007). Concentrations of O_3 at background locations in Europe have been increasing during the last few decades (Lelieveld et al., 2004; Derwent et al., 2007) although the observed trend has weakened in the first years of the 21st century (Isaksen et al., 2009). A similar increase is also observed in the boundary layer air inflow at the west coast of North America (Parrish et al., 2009). To assess the importance of continued increase of background O_3 we performed one simulation where the background concentration of O_3 increase by 0.1 ppb(v) yr^{-1} from 1990 to 2100. This is a weaker trend than has been observed during recent decades at Mace Head (Derwent et al., 2007) but still implies a substantial increase of background O_3 of 5 ppb(v) over the period 2000–2050. In

Table 1. Modelled surface O_3 compared to observed values over the years 1990–2009 at EBAS stations in Europe[a].

	Observation ppb(v)	Model ppb(v)	bias %	spatial correlation	RMSE ppb(v)	#stations
	April–September mean					
North of 50° N	31.7	33.8	6.8	0.06	4.8	45
South of 50° N	37.8	38.1	0.9	0.58	5.4	49
	April–September mean of daily max					
North of 50° N	42.4	41.4	−2.3	0.61	3.5	45
South of 50° N	52.1	48.6	−6.6	0.58	5.3	49

[a] Modelled (Increasing boundary case, ECH_RCP4.5_BCtrend) and measured average values at EBAS sites were constructed for years with measurement data capture exceeding 75 % to account for trend in emissions and observed trend in hemispheric background. Sites at an elevation deviating more than 250 m from the model height were excluded from the evaluation. Model data were taken from the level 3 m above surface.

this experiment we also allow the concentration of CH_4 to vary according to the concentration pathway provided by the RCP4.5 scenario. This means that the global average concentration of CH_4 increases to a maximum of 1842 ppb(v) in 2040 and then drops to 1576 ppb(v) in 2100.

2.5 Model evaluation

To evaluate the performance of the MATCH-RCA3 modelling system, we compare our "Increasing boundary case" (see below) to measured O_3 concentrations for 1990–2009. The observations were extracted from the EBAS data base (http://ebas.nilu.no). The results of the evaluation are displayed in Table 1. The O_3 measures compared are daily mean and daily maximum averages, for the summer half year for stations north and south of 50° N respectively. In the evaluation we accounted for the fact that the emissions of ozone precursors change over time during 1990–2009 by forming and comparing station-averages only during those years with valid observations. The number of stations given in Table 1 refers to the total number of stations used in each part of the domain. The requirement for including a station apart from the elevation difference criteria was a 75 % data capture for each year. In the north and south, 82 and 69 % respectively of the included stations had more than 10 yr of valid data. The present setup of the modelling system shows comparable performance as earlier applications of MATCH using climate model output (e.g. Langner et al., 2005; Andersson and Engardt, 2010), but the spatial correlation is not as good. Part of the difference can be related to differences in climate simulated by the GCMs used in the different studies. Evaluation of MATCH driven by meteorological data constrained by observations shows better correlation. For example, evaluation of a 7-yr simulation with MATCH for the period 1997–2003 using ERA40 as meteorological input has been presented by Andersson et al. (2009). The correlation for the whole domain was in this case 0.61 for mean values and 0.87 for daily max values which are better than what we obtained in

the present study which are 0.55 and 0.71 respectively. It is important to note that the comparison is sensitive to which simulated time period that is used in the comparison, due to long-term (decadal) variations in the simulated climate that do not necessarily coincide with the observed meteorology. The spatial correlation for average ozone north of 50° N is particularly low while it is higher to the south and also higher for average of daily maximum. The bias and RMSE for mean O_3 in north Europe is comparable to the values in south Europe and for mean of daily maximum. The low spatial correlation for average ozone in the north could partly be due to biases in the simulation of current climate in the global climate projection from ECHAM5. However, the scores using meteorological data downscaled from HadCM3 show similar low values for northern Europe, with a correlation of 0.02 and a bias of 12.4 % for summer mean concentrations of O_3.

3 Results and discussion

In this section we discuss the results from four MATCH simulations covering the period 1990–2100:

1. Climate sensitivity case 1 (ECH_RCP2000_BC2000); describing the effect of changing climate (downscaled ECHAM5) on surface O_3. Boundary concentration of CH_4 and O_3, and anthropogenic precursor emissions are kept at the level of year 2000.

2. Climate sensitivity case 2 (HAD_RCP2000_BC2000); modelling set up as in case 1, but simulated with another climate projection (downscaled HadCM3).

3. Emission reduction case (ECH_RCP4.5_BC2000); where anthropogenic O_3 precursor emissions in Europe follow RCP4.5, while background concentrations of O_3 and CH_4 are kept at the level of year 2000. The climate projection downscaled from ECHAM5 is used in this case.

Table 2. Model simulated 20-yr mean surface O_3 and variability[a] during different periods over the European land area.

	April–September daily max				April–September mean			
	1990–2009	2040–2059	2080–2099	1990–2099	1990–2009	2040–2059	2080–2099	1990–2100
North of 50° N		ppb(v)		ppb(v) century^{-1}		ppb(v)		ppb(v) century^{-1}
ECH_RCP2000_BC2000	40	39	39	−0.5	32	32	32	−0.5
HAD_RCP2000_BC2000	42	41	41	−0.8	33	33	33	−0.8
ECH_RCP4.5_BC2000	40	34	32	−9.2	32	28	26	−7.2
ECH_RCP4.5_BCtrend	40	36	35	−5.0	32	30	29	−3.8
South of 50° N								
ECH_RCP2000_BC2000	50	51	53	3.5	38	39	40	2.1
HAD_RCP2000_BC2000	51	52	54	3.2	39	40	40	1.9
ECH_RCP4.5_BC2000	50	41	38	−12.8	39	32	30	−9.5
ECH_RCP4.5_BCtrend	50	43	41	−9.7	38	33	32	−7.1
North of 50° N			variability ppb(v)					
ECH_RCP2000_BC2000	1.9	2.2	2.7		1.7	1.5	2.1	
HAD_RCP2000_BC2000	1.8	2.6	1.9		1.4	2.0	1.5	
ECH_RCP4.5_BC2000	3.3	2.2	1.6		2.4	1.8	1.3	
ECH_RCP4.5_BCtrend	3.0	1.7	1.8		2.1	1.6	1.5	
South of 50° N								
ECH_RCP2000_BC2000	2.4	4.3	6.2		1.4	2.3	3.5	
HAD_RCP2000_BC2000	2.9	6.0	5.3		1.6	3.3	2.9	
ECH_RCP4.5_BC2000	5.7	3.7	4.2		3.2	2.5	3.0	
ECH_RCP4.5_BCtrend	5.2	3.7	4.5		2.8	2.4	3.2	

[a] Variability is defined as the difference between the highest and lowest summer mean value in each 20-yr period. Trends are from linear regressions over the period 1990–2100.

4. Increasing boundary case (ECH_RCP4.5_BCtrend); including varying anthropogenic precursor emissions in Europe according to RCP4.5, increasing background ozone with $0.1\,\mathrm{ppb(v)\,yr^{-1}}$ and changing CH_4 concentrations following RCP4.5. The climate projection downscaled from ECHAM5 is used in this case.

Figure 1a and b show the temporal evolution of summer mean and summer mean of daily max O_3 for the four simulations averaged over the European land area north and south of 50° N, respectively.

The upper two lines in each four-line group correspond to the two climate sensitivity cases (ECH_RCP2000_BC2000 and HAD_RCP2000_BC2000). Here we kept the O_3 precursor emissions and boundary concentrations constant over time at their year 2000 values to isolate the effect of meteorological changes. For northern Europe we note a slight downward trend for daily max (−0.5 and −0.8 ppb(v) century^{-1} for ECH_RCP2000_BC2000 and HAD_RCP2000_BC2000 respectively) with small inter-annual variability. Trends over the whole period are given in Table 2. In southern Europe there are increases in surface O_3 over time for the climate sensitivity cases. The variability in the simulations are different for different time periods, but the trends in the two simulations are similar (+3.5 and +3.2 ppb(v) century^{-1} for daily max). Earlier studies using the MATCH model have shown that two main drivers for the increasing summer surface O_3 in southern Europe are decrease in dry deposition of O_3 due to reduced soil water and thereby reduced vegetation uptake,

and increase in biogenic isoprene emissions, with decrease in dry deposition being the dominant effect in the southernmost parts of Europe and both being equally important in central Europe (Andersson and Engardt, 2010). The reasons for the reduced concentrations in northern Europe have not been addressed in detail here but both cloudiness and precipitation increase in northern Europe in the climate projections which should lead to increased scavenging of ozone precursors and less solar radiation for driving the photochemistry. It is interesting to note the substantial decadal variability in the trend of surface O_3 especially in southern Europe. For example, during the period 2020 to 2030 climate variability leads to decreasing surface O_3 in southern Europe in both the ECH_RCP2000_BC2000 and HAD_RCP2000_BC2000 simulation, with a more prominent decrease in the latter case.

When we include also the change in ozone precursor emissions in Europe following the RCP4.5 scenario (ECH_RCP4.5_BC2000) we obtain decreasing surface O_3 concentrations across Europe. The impact of reduced emissions in Europe clearly dominates over climate change impacts and leads to reductions of daily max O_3 both in northern and southern Europe until 2100 (−9.2 and −12.8 ppb(v) century^{-1}, respectively). Applying a potential trend of background O_3 of +0.1 ppb(v) yr^{-1} (ECH_RCP4.5_BCtrend) results in partial cancellation of the O_3 decrease due to emission changes in – especially northern – but also southern Europe. The resulting change in surface daily max O_3 from 1990 to 2100 in these regions now become −5.0

and $-9.7\,\mathrm{ppb(v)}$ century^{-1}, respectively. The current model setup is less well suited to model ozone trends during 1990–2009 since the meteorological data used to drive the CTM simulations are taken from climate model output. Trends in meteorological variables in the simulation are therefore not necessarily in phase with observed changes.

Due to substantial year to year variability in the simulations it is important to study averages over sufficiently long time periods in order to find statistically significant changes. We use climate projections from two global climate models to account for some of the uncertainty in simulating future climate change. Although the long-term trend in the two simulations is similar differences for shorter periods can be large as a reflection of the inherent variability in the climate system. Table 2 summarizes 20-yr average concentrations and variability for northern and southern Europe over the periods 1990–2009 and 2040–2059 and 2080–2099. The absolute variability is larger in southern Europe than in northern and it increases with time in the climate sensitivity case based on ECHAM5. When using HadCM3 the variability first increases and then decreases. The opposite is seen in the Emission reduction case and Increasing boundary case. The decrease in variability until mid-century is probably due to decreasing emissions whereas the increasing variability in the ECHAM5 downscaling cause further variability beyond this point as can be seen throughout the century in the Increasing boundary case.

Figure 2 shows the current and future frequency distributions of O_3 concentrations in northern and southern Europe for the Increasing boundary case and for the Climate sensitivity case 1. For the Increasing boundary case we observe that there is a shift over time of the peak of the distribution to lower concentrations, the shift being slightly smaller for northern Europe than for southern Europe. For high concentrations we note larger changes in the frequency distribution both in northern and southern Europe. This shows that emission reductions within Europe are especially effective in reducing the highest O_3 concentrations connected to O_3 episodes also in northern Europe although the overall average is only reduced slightly due to increasing background concentrations. When considering only climate change (keeping emissions and lateral boundaries at their ca. 2000 values), the trends in the frequency distributions are quite different. The peaks of the distributions remain unchanged in both Northern and Southern Europe. For southern Europe, the high end tail of the distribution is, however clearly increased during the period 2040–2059 compared to 1990–2009. This feature is also seen in northern Europe, but to a lesser extent. The implication is that climate change increases the peak values of surface ozone.

The spatial distributions of the changes in mean and daily max O_3 between the periods 1990–2009 and 2040–2059 for the four simulations are shown in Figs. 3 and 4 respectively. Climate change alone increases O_3 in southern Europe in both the climate sensitivity simulations. The increase is gen-
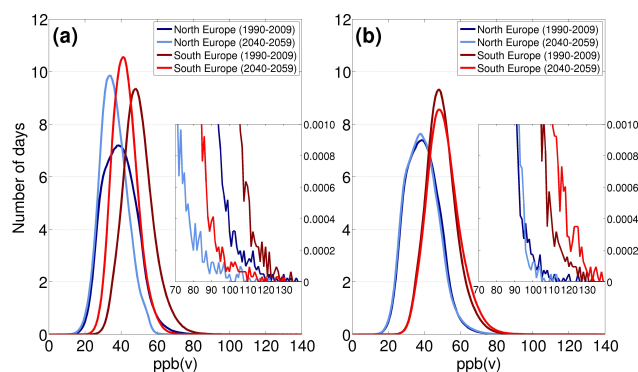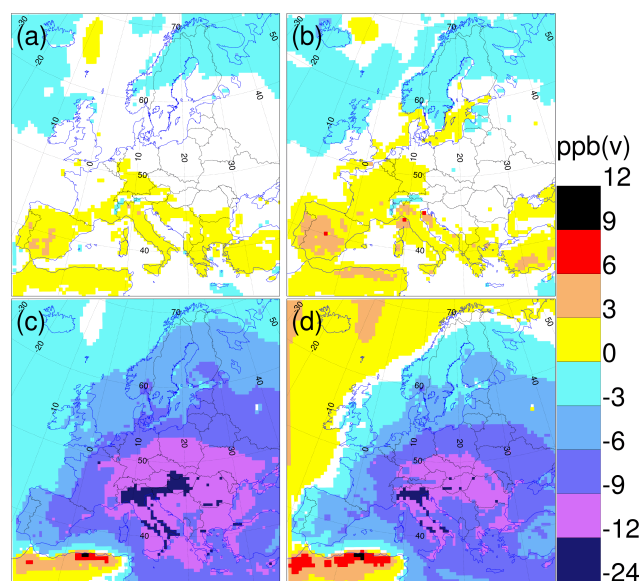

Fig. 2. Frequency distributions of daily max O_3 concentrations in North and South Europe during the periods 1990–2009 and 2040–2059 in the Increasing boundary case simulation **(a)** and Climate sensitivity case 1 **(b)**. The distributions show the number of days per year one arbitrary model grid point in northern and southern Europe experiences daily maximum O_3 concentrations between X and $X+1$ ppb(v) during the respective 20-yr period.

erally in the range 0–3 ppb(v) for summer mean. Decrease of 0–3 ppb(v) in summer mean O_3 is simulated in the northern part of the model domain. Changes for summer mean of daily max are somewhat larger, 3–6 ppb(v), in regions of southern Europe, while the reductions in the northern part of the model domain are still in the range 0–3 ppb(v). Increases are somewhat larger when using the HadCM3 projection and also cover larger areas of north-western Europe. When including the trend in RCP4.5 anthropogenic precursor emissions reductions of O_3 are evident everywhere except in northern Africa were O_3 precursor emissions are increasing until 2040 in RCP4.5 and for a few grid points close to Helsinki and Moscow. In these urban areas the reductions in NO$_x$ emissions lead to a reduced loss of O_3 through reaction with NO and increasing O_3 concentrations locally. For mean O_3 the effect is visible also for a few other locations in the northern part of Europe, e.g. London and Amsterdam while the effect is not visible further south. This is related to differences in photochemical regimes in different parts of Europe with more NO$_x$ sensitive regimes in northern Europe (Beekman and Vautard, 2010). Reductions exceed 9 ppb(v) for summer mean and 12 ppb(v) for summer daily max in a region extending from northern Italy to Hungary. For the Increasing boundary case the assumed upward trend in background O_3 clearly impacts the concentration along the western and northern part of the model domain. The change over the North Atlantic and the British Isles is reversed from negative to positive compared to the scenario with constant boundaries, with net O_3 changes now of 0 to +3 ppb(v) on the British Isles for daily mean. However, most parts of the European land areas still experiences decreasing mean O_3. Corresponding changes in daily max O_3 have a similar geographical pattern, but smaller magnitude.
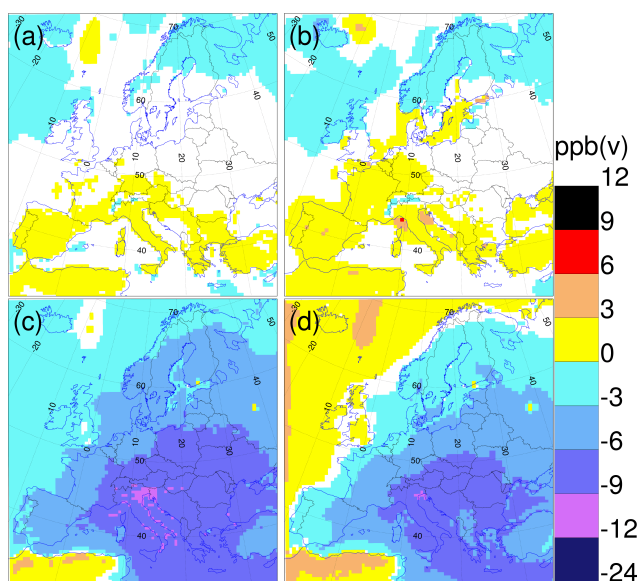
Fig. 3. Change in summer (April–September) mean surface O_3 concentration from 1990–2009 to 2040–2059. **(a)** and **(b)** changes due to change in climate only; RCA3 downscaling of ECHAM5 and HadCM3, respectively. **(c)** ECHAM5 downscaling and change in European O_3 precursor emissions. **(d)** Increasing boundary case; the combined change due to change in climate, change in O_3 precursor emissions and an increasing hemispheric background of O_3 of 0.1 ppb(v) yr^{-1}. Non-significant changes at 95% confidence level are masked white.

Fig. 4. Change in summer (April–September), daily maximum, surface O_3 concentration from 1990–2009 to 2040–2059. **(a)** and **(b)** changes due to change in climate only; RCA3 downscaling of ECHAM5 and HadCM3, respectively. **(c)** ECHAM5 downscaling and change in European O_3 precursor emissions. **(d)** Increasing boundary case; the change due to combined change in climate, change in O_3 precursor emissions and an increasing hemispheric background of O_3 of 0.1 ppb(v) yr^{-1}. Non-significant changes at 95 % confidence level are masked white.

It is clear from the results presented above that the future evolution of background tropospheric O_3 in the northern hemisphere will be important for the resulting surface O_3 concentration in large parts of Europe. Wild et al. (2012) present estimates of regional changes of surface O_3 based on average source receptor calculations with 14 different global models for present (2001) meteorological and emission conditions. They estimate that changes in annual mean O_3 between 2000 and 2050 averaged over Europe would be negative for all RCP scenarios except for RCP 8.5 which has the largest increase of greenhouse gases. The changes are substantially different than estimated with the SRES A1B, A2 and B2 scenarios, reflecting the assumptions of more stringent O_3 precursor emission controls under the RCP scenarios. Domain and annual average changes in mean O_3 in our Increasing boundary case is -0.2 ppb(v) which can be compared to -2.7 and $+0.3$ ppb(v) estimated by Wild et al. (2012) for RCP4.5 and 8.5 respectively. The change in our Emission reduction case, which assumes that background O_3 is unchanged around Europe, is -2.5 ppb(v) which is similar to the total change given by Wild et al. (2012) for RCP 4.5 but it is somewhat larger than the change they estimate due to reduction in European precursor emissions for RCP 8.5 and 2.6, which are about -1.5 to -2 ppb(v). It should be noted that the European domains used in these calculations are not identical; the domain used by Wild et al. (2012) being larger

and shifted to the east and south. For the summer period the decrease is much larger, -2.4 and -4.3 ppb(v) for our Increasing boundary case and Emission reduction case respectively, illustrating that the reduction in European O_3 precursor emissions are much more important in summer than in the annual mean.

4 Conclusions

We have studied the impact of climate change and changes in O_3 precursor emissions on summer time surface O_3 over Europe using two different projections of global climate from the SRES A1B scenario and the combined effect of also including ozone precursor emission changes under the RCP4.5 scenario over the period 1990 to 2100. The following conclusions can be drawn:

1. In southern Europe regional climate change gives a substantial positive contribution to future surface O_3 concentrations, but emission reductions are more important leading to reduced O_3 concentrations, also when including increasing hemispheric background concentrations.

2. In northern Europe regional climate change decreases surface O_3 and reduced emissions acts to further

strengthen this trend also when including increasing hemispheric background concentrations.

3. The sensitivity to regional climate change using climate projections from two global climate models gave similar spatial changes in surface O_3 and similar long-term temporal trends although the trends differ between different periods.

4. There is substantial decadal variability in the simulations, forced by climate variability, which is important to consider when looking at changes in concentrations of surface O_3, especially until the first half of the 21st century.

Conclusion 1 and 2 is dependent on our use of the RCP4.5 emission scenario for O_3 precursors in Europe which assumes substantial air pollution abatement measures. It remains to be seen if these reductions can be achieved. In this study we have used a regional CTM coupled to a regional climate model to simulate details in changes of surface O_3 over Europe over long time periods. A drawback with this model setup is that assumptions have to be made about trends in the concentrations of chemical components on the model boundaries. This means that possible future changes in stratosphere-troposphere exchange, lightning NO_x and O_3 loss due to increasing water vapour on the global scale are only implicitly accounted for through an assumed trend on the model boundaries. In an ensemble analysis of 10 global GCM-CTMs the combined effect of these processes on background surface ozone in the northern hemisphere was estimated to -0.8 ± 0.7 ppb(v) for 2000–2030 climate change by Dentener et al. (2006). Additional potentially important missing processes/feedbacks include change in vegetation/land use and change in wild fire emissions. The study of the importance of land use changes is still in an early stage. In a global model study Ganzeveld et al. (2010) simulated changes in boundary layer O_3 on the order of $+2\%$ between 2000 and 2050 in southern Europe. Ultimately the spatial resolution of global CTMs will be adequate to simulate also regional details of surface O_3. Until then coupling of global (hemispheric) and regional CTMs forced by a consistent set of meteorological data and precursor emissions is a useful way forward.

Edited by: P. Monks

References

Amann, M., Imrich, B., Cofala, J., Heyes, C., Klimont, Z., Rafaj, P., Schöpp, W., and Wagner, F.: Scope for further environmental improvements in 2020 beyond the baseline projections. Background paper for the 47th Session of the Working Group on Strategies and Review of the Convention on Long-range Transboundary Air Pollution Geneva, 30 August–3 September 2010, Centre for Integrated Assessment Modelling (CIAM) International Institute for Applied Systems Analysis (IIASA) CIAM Report 1/2010, 2010.

Andersson, C., Bergström, R., and Johansson, C.: Population exposure and mortality due to regional background PM in Europe – long-term simulations of source-region and shipping contributions, Atmos. Environ., 43, 3614–3620, 2009.

Andersson, C. and Engardt, M.: European ozone in a future climate – The importance of changes in dry deposition and isoprene emissions, J. Geophys. Res., 115, D02303, doi:10.1029/2008JD011690, 2010.

Andersson, C., Langner, J., and Bergström, R.: Interannual variation and trends in air pollution over Europe due to climate variability during 1958-2001 simulated with a regional CTM coupled to the ERA40 reanalysis, Tellus B, 59, 77–98, 2007.

Beekmann, M. and Vautard, R.: A modelling study of photochemical regimes over Europe: robustness and variability, Atmos. Chem. Phys., 10, 10067–10084, doi:10.5194/acp-10-10067-2010, 2010.

Collins, M., Booth, B. B. B., Bhaskaran, B., Harris, G. R., Murphy, J. M., Sexton, D. M. H., and Webb, M. J.: Climate model errors, feedbacks and forcings: a comparison of perturbed physics and multi-model ensembles, Clim. Dynam., 36, 1737–1766, doi:10.1007/s00382-010-0808-0, 2010.

Dentener, F., Stevenson, D., Ellingsen, K., van Noije, T., Schultz, M., Amann, M., Atherton, C., Bell, N., Bergmann, D., Bey, I., Bouwman, L., Butler, T., Cofala, J., Collins, B., Drevet, J., Doherty, R., Eickhout, B., Eskes, H., Fiore, A., Gauss, M., Hauglustaine, D., Horowitz, L., Isaksen, I. S. A., Josse, B., Lawrence, M., Krol, M., Lamarque, J. F., Montanaro, V., Müller, J. F., Peuch, V. H., Pitari, G., Pyle, J., Rast, S., Rodriguez, J., Sanderson, M. Savage, N. H., Shindell, D., Strahan, S., Szopa, S., Sudo, K., Van Dingenen, R., Wild, O., and Zeng, G.: The global atmospheric environment for the next generation, Environ. Sci. Technol., 40, 3586–3594, doi:10.1021/es0523845, 2006.

Derwent, R. G., Simmonds, P. G., Manning, A. J., and Spain, T. G.: Trends over a 20-year period from 1987 to 2007 in surface ozone at the atmospheric research station, Mace Head, Ireland, Atmos. Environ., 41, 9091–9098, 2007.

Engardt, M., Bergström, R., and Andersson, C.: Climate and emission changes contributing to changes in near-surface ozone in Europe over the coming decades: Results from model studies, Ambio, 38, 452–458, 2009.

Fiore, A. M., Naik, V., Spracklen, D., Steiner, A., Unger, N., Prather, M., Bergmann, D., Cameron-Smith, P. J., Collins, B., Dalsøren, S., Folberth, G., Ginoux, P., Horowitz, L.W., Josse, B., Lamarque, J.-F., Nagashima, T., O'Connor, F., Rumbold, S., Shindell, D. T., Skeie, R. B., Sudo, K., Takemura, T., and Zeng, G.: Global Air Quality and Climate, Chem. Soc. Rev., 41, 6663–6683, doi:10.1039/c2cs35095e, 2012.

Ganzeveld, L., Bouwman, L., Stehfest, E., van Vuuren, D. P., Eickhout B., and Lelieveld, J.: Impact of future land use and land cover changes on atmospheric chemistry-climate interactions, J.

Geophys. Res., 115, D23301, doi:10.1029/2010JD014041, 2010.

Isaksen, I. S. A., Granier, C., Myhre, G., Berntsen, T. K., Dalsøren, S. B., Gauss, M., Klimont, Z., Benestad, R., Bousquet, P., Collins, W., Cox, T., Eyring, V., Fowler, D., Fuzzi, S., Jöckel, P., Laj, P., Lohmann, U., Maione, M., Monks, P., Prevot, A.S.H., Raes, F., Richter, A., Rognerud, B., Schulz, M., Shindell, D., Stevenson, D. S., Storelvmo, T., Wang, W.-C., van Weele, M., Wild, M., and Wuebbles, D.: Atmospheric Composition Change: Climate-Chemistry interactions, Atmos. Environ., 43, 5138–5192, 2009.

Jacob, D. J. and Winner, D. A.: Effect of climate change on air quality, Atmos. Environ., 43, 51–63, 2009.

Katragkou, E., Zanis, P., Kioutsioukis, I., Tegoulias, I., Melas, D., Krüger, B. C., and Coppola, E.: Future climate change impacts on summer surface ozone from regional climate-air quality simulations over Europe, J. Geophys. Res., 116, D22307, doi:10.1029/2011JD015899, 2011.

Kjellström, E., Nikulin, G., Hansson, U., Strandberg, G., and Ullerstig, A.: 21st century changes in the European climate: uncertainties derived from an ensemble of regional climate model simulations, Tellus, 63A, 24–40, doi:10.1111/j.1600-0870.2010.00475.x, 2011.

Lamarque, J.-F., Bond, T. C., Eyring, V., Granier, C., Heil, A., Klimont, Z., Lee, D., Liousse, C., Mieville, A., Owen, B., Schultz, M. G., Shindell, D., Smith, S. J., Stehfest, E., Van Aardenne, J., Cooper, O. R., Kainuma, M., Mahowald, N., McConnell, J. R., Naik, V., Riahi, K., and van Vuuren, D. P.: Historical (1850–2000) gridded anthropogenic and biomass burning emissions 25 of reactive gases and aerosols: methodology and application, Atmos. Chem. Phys., 10, 7017–7039, doi:10.5194/acp-10-7017-2010, 2010.

Langner, J., Bergström, R., and Foltescu, V.: Impact of climate change on surface ozone and deposition of sulphur and nitrogen in Europe, Atmos. Environ., 39, 1129–1141, 2005.

Lelieveld, J., van Aardenne, J., Fischer, H., de Reus, M., Williams J., and Winkler, P.: Increasing Ozone over the Atlantic Ocean, Science, 304, 1483–1487, doi:10.1126/science.1096777, 2004.

Meleux, F., Solmon, F., and Giorgi, F.: Increase in summer European ozone amounts due to climate change, Atmos. Environ., 41, 7577–7587, doi:10.1016/j.atmosenv.2007.05.048, 2007.

Nakićenović, N., Alcamo, J., Davis, G., de Vries, B., Fenhann, J., Gaffin, S., Gregory, K., Grübler, A., Yong Jung, T., Kram, T., La Rovere, E. L., Michaelis, L., Mori, S., Morita, T., Pepper, W., Pitcher, H., Price, L., Riahi, K., Roehrl, A., Rogner, H.-H., Sankovski, A., Schlesinger, M., Shukla, P., Smith, S., Swart, R., van Rooijen, S., Victor, N., and Dadi, Z.: Emission scenarios, A special report of working group III of the Intergovernmental Panel on Climate Change, Cambridge University Press, 2000.

Parrish, D. D., Millet, D. B., and Goldstein, A. H.: Increasing ozone in marine boundary layer inflow at the west coasts of North America and Europe, Atmos. Chem. Phys., 9, 1303–1323, doi:10.5194/acp-9-1303-2009, 2009.

Robertson, L., Langner, J., and Engardt, M.: An Eulerian limited-area atmospheric transport model, J. Appl. Meteorol., 38, 190–210, 1999.

Roeckner, E., Brokopf, R., Esch, M., Giogietta, M., Hagemann, S., Kornblueh, L., Manzini, E., Schlese, U., and Schulzweida, U.: Sensitivity of simulated climate to horizontal and vertical resolutions in the ECHAM5 atmosphere model, J. Climate, 19, 3771–3791, doi:10.1175/JCLI3824.1, 2006.

Royal Society: Ground-level Ozone in the 21st Century: Future Trends, Impacts and Policy Implications, Science Policy Report 15/08, Royal Society, London, 2008.

Samuelsson, P., Jones, C. G., Willén, U., Ullerstig, A., Gollvik, S., Hansson, U., Jansson, C., Kjellström, E., Nikulin, G., and Wyser, K.: The Rossby Centre Regional Climate model RCA3: Model description and performance, Tellus A, 63, 4–23, doi:10.1111/j.1600-0870.2010.00478.x, 2011.

Simpson, D., Andersson-Sköld, Y., and Jenkin, M. E.: Updating the chemical scheme for the EMEP MSC-W oxidant model: Current status, EMEP MSC-W Note 2/93, Norwegian Meteorological Institute, Oslo, 1993.

Simpson, D., Guenther, A., Hewitt, C. N., and Steinbrecher, R.: Biogenic emissions in Europe: 1. Estimates and uncertainties, J. Geophys. Res., 100, 22875–22890, doi:10.1029/95JD02368, 1995.

Thomson, A. M., Calvin, K. V., Smith, S. J., Kyle, G. P., Volke, A., Patel, P., Delgado-Arias, S., Bond-Lamberty, B., Wise, M. A., Clarke, L. E., and Edmonds, J. A.: RCP4.5: a pathway for stabilization of radiative forcing by 2100, Climatic Change, 109, 77–94, doi:10.1007/s10584-011-0151-4, 2011.

Wild, O., Fiore, A. M., Shindell, D. T., Doherty, R. M., Collins, W. J., Dentener, F. J., Schultz, M. G., Gong, S., MacKenzie, I. A., Zeng, G., Hess, P., Duncan, B. N., Bergmann, D. J., Szopa, S., Jonson, J. E., Keating T. J., and Zuber, A.: Modelling future changes in surface ozone: a parameterized approach, Atmos. Chem. Phys., 12, 2037–2054, doi:10.5194/acp-12-2037-2012, 2012.